

attributable to the interference of the two chlorine atoms in cis positions. These adjacent Cl atoms not only provide strong steric interaction but also electrostatic repulsion.

Acknowledgment. We are grateful to Dr. M. T. Wu of the Department of Chemistry, Chun Shan Institute of Science and Technology, for the help of data collection on a Nonius CAD-4F diffractometer. This work has been financially

supported in part by the National Science Council, Republic of China.

Registry No. I, 70787-84-7.

Supplementary Material Available: Tables of anisotropic thermal parameters of nonhydrogen atoms and structure factor amplitudes for I (6 pages). Ordering information is given on any current masthead page.

Contribution from the Department of Chemistry,
University of Wisconsin—Madison, Madison, Wisconsin 53706

Synthesis, Chemistry, and Low-Temperature Crystal and Molecular Structure of $[\mu-(\eta^5\text{-Cyclopentadienyl})\text{beryllio}]_{\text{octahydropentaborane}}, [\mu-(\eta^5\text{-C}_5\text{H}_5)\text{Be}]_{\text{B}_5\text{H}_8}$

DONALD F. GAINES,* KRAIG M. COLESON, and JOSEPH C. CALABRESE

Received December 2, 1980

Reaction of $(\eta^5\text{-C}_5\text{H}_5)\text{BeCl}$ with KB_5H_8 results in formation of the title compound, which forms crystals in the monoclinic space group $P2_1/c$ with $a = 10.266$ (8) Å, $b = 5.616$ (4) Å, $c = 16.187$ (7) Å, $\beta = 98.50$ (5)°, $V = 923.0$ (5) Å³, and $Z = 4$. The low-temperature X-ray structure was solved by direct methods, using anisotropic refinement of positional and temperature factors for nonhydrogen atoms and isotropic refinement for hydrogen atoms, which converged to $R_1 = 0.0551$ and $R_2 = 0.0831$ for 1294 independent observed reflections. The structure of $[\mu-(\eta^5\text{-C}_5\text{H}_5)\text{Be}]_{\text{B}_5\text{H}_8}$ is like that of B_5H_9 , but with a bridge hydrogen replaced by the $(\eta^5\text{-C}_5\text{H}_5)\text{Be}$ moiety. Selected chemical properties of the title compound are described.

Introduction

Beryllium, in the form of $\text{Be}(\text{BH}_4)_2$, may be inserted into a borane cluster by reaction with $1\text{-ClB}_5\text{H}_8$ to produce 2-berylla-2-(tetrahydroborato)hexaborane(11),¹ $\text{B}_5\text{H}_{10}\text{BeBH}_4$, which has a six-vertex pentagonal-pyramidal $\text{B}_5\text{-Be}$ cluster framework.² The mechanism of this reaction is complex, and $\text{Be}(\text{BH}_4)_2$ presents some handling difficulties. Thus other synthetic routes to beryllaborane clusters are desirable. The successful insertion of boron, as $(\text{CH}_3)_2\text{BCl}$, into a bridging position in pentaborane(9) and subsequent rearrangement to a hexaborane(10) derivative³ (eq 1) suggested that a similar $\text{LiB}_5\text{H}_8 + (\text{CH}_3)_2\text{BCl} \rightarrow [\mu\text{-(CH}_3)_2\text{B}]_{\text{B}_5\text{H}_8} \rightarrow 2,3\text{-(CH}_3)_2\text{B}_6\text{H}_8$ (1)

insertion might occur with use of selected beryllium compounds. We present here the results of our initial investigations of such a beryllium-insertion reaction, in which $(\eta^5\text{-C}_5\text{H}_5)\text{BeCl}$ was used as the insertion reagent.

Results and Discussion

The reaction of $(\eta^5\text{-C}_5\text{H}_5)\text{BeCl}$ with KB_5H_8 in a pentane slurry at ca. -40 °C produces good yields of $[\mu-(\eta^5\text{-C}_5\text{H}_5)\text{Be}]_{\text{B}_5\text{H}_8}$ according to eq 2. The product is a colorless solid $\text{KB}_5\text{H}_8 + (\eta^5\text{-C}_5\text{H}_5)\text{BeCl} \rightarrow \text{KCl} + [\mu-(\eta^5\text{-C}_5\text{H}_5)\text{Be}]_{\text{B}_5\text{H}_8}$ (2)

of low volatility that melts at ca. 38 °C. Characterization of the product was accomplished initially via mass and NMR spectroscopy, and the detailed structural parameters were obtained from a single-crystal X-ray study.

The ambient ¹¹B FT NMR spectrum of $[\mu-(\eta^5\text{-C}_5\text{H}_5)\text{Be}]_{\text{B}_5\text{H}_8}$ is appropriate for a μ -substituted B_5H_9 derivative. It consists of three doublets of intensity 2:2:1 at $\delta -13.4$ ($J = 161$ Hz), -21.8 ($J = 141$ Hz), and -54.6 ($J = 170$ Hz), respectively. With ¹H decoupled, ¹¹B(apex)-¹¹B(base) coupling is observed in both sets of basal boron resonances.

Table I. Interatomic Distances (Å) for $[\mu-(\eta^5\text{-C}_5\text{H}_5)\text{Be}]_{\text{B}_5\text{H}_8}$

C(1)-C(2)	1.391 (3)	B(2)-B(5)	1.812 (3)
C(1)-C(5)	1.397 (3)	B(2)-H(2)	1.102 (20)
C(1)-H(6)	0.931 (22)	B(2)-H(5-2)	1.263 (20)
C(2)-C(3)	1.398 (3)	B(1)-B(2)	1.696 (3)
C(2)-H(7)	0.929 (24)	B(1)-B(3)	1.705 (3)
C(5)-H(4)	1.401 (3)	B(1)-B(4)	1.675 (3)
C(5)-H(10)	1.045 (24)	B(1)-B(5)	1.663 (3)
C(4)-C(3)	1.396 (4)	B(1)-H(1)	0.980 (25)
C(4)-H(9)	0.980 (33)	B(3)-B(4)	1.821 (3)
C(3)-H(8)	0.899 (27)	B(3)-H(3)	1.041 (20)
Be(1)-C(1)	1.886 (3)	B(3)-H(3-4)	1.268 (20)
Be(1)-C(2)	1.894 (3)	B(4)-B(5)	1.799 (3)
Be(1)-C(5)	1.892 (3)	B(4)-H(4)	1.039 (20)
Be(1)-C(4)	1.877 (3)	B(4)-H(3-4)	1.251 (22)
Be(1)-C(3)	1.884 (3)	B(4)-H(4-5)	1.242 (21)
Be(1)-B(2)	2.045 (3)	B(5)-H(5)	1.065 (27)
Be(1)-B(3)	2.055 (3)	B(5)-H(4-5)	1.293 (20)
B(2)-B(3)	1.726 (3)	B(5)-H(5-2)	1.310 (21)

the most interesting feature of the ¹¹B NMR spectrum is the large upfield shift of the resonances associated with two of the basal borons, suggesting a higher concentration of electron density, while the other chemical shifts are not significantly different from those of B_5H_9 . It is interesting to note that the average of the chemical shifts for the two sets of basal boron resonances of $[\mu-(\eta^5\text{-C}_5\text{H}_5)\text{Be}]_{\text{B}_5\text{H}_8}$ is the same as that observed for B_5H_8^- salts.³ The static structure, solubility in hydrocarbons, and volatility, however, confirm the covalency of the B-Be-B bonding. The 270-MHz ¹H FT NMR spectrum contains a sharp singlet at $\delta 5.4$ (C_5H_5), quartets at $\delta 2.7$, 1.8 , and 1.1 ($\text{B}_1\text{-H}$) for the terminal B-H's, and broad singlets of intensity 1:2 at $\delta -2.5$ and -3.7 , respectively, for the bridging hydrogens.

The X-ray determined structure of $[\mu-(\eta^5\text{-C}_5\text{H}_5)\text{Be}]_{\text{B}_5\text{H}_8}$ is shown in Figure 1. The internuclear distances and angles are given in Tables I and II, respectively. Some interesting features appeared in the structural data which were not discernible from the NMR data. The shortening of the B(2)-B(3) distance (Table I) suggests a higher concentration of electron density in this region in agreement with the assignment of the higher field resonance in the ¹¹B NMR spectrum to the borons adjacent to beryllium. The tilt of H(4,5) under

(1) Gaines, D. F.; Walsh, J. L. *J. Chem. Soc., Chem. Commun.* 1976, 482; *Inorg. Chem.* 1978, 17, 1238.

(2) Gaines, D. F.; Walsh, J. L.; Calabrese, J. C. *Inorg. Chem.* 1978, 17, 1242.

(3) Gaines, D. F.; Iorns, T. V. *J. Am. Chem. Soc.* 1970, 92, 4571-4574.

Table II. Intramolecular Angles (Deg) for $[\mu-(\eta^5\text{-C}_5\text{H}_5)\text{Be}]_2\text{B}_5\text{H}_8$

C(2)-C(1)-C(5)	108.7 (2)	B(2)-B(5)-B(4)	89.1 (5)
C(2)-C(1)-Be(1)	68.7 (1)	B(2)-B(5)-H(5)	136.3 (15)
C(2)-C(1)-H(6)	124.6 (13)	B(2)-B(5)-H(4-5)	103.8 (9)
C(5)-C(1)-Be	68.5 (1)	B(2)-B(5)-H(2-5)	44.2 (9)
C(5)-C(1)-H(6)	126.4 (13)	B(4)-B(5)-H(5)	134.3 (15)
Be(1)-C(1)-H(6)	123.9 (13)	B(4)-B(5)-H(4-5)	43.7 (9)
C(1)-C(2)-C(3)	107.7 (2)	B(4)-B(5)-H(2-5)	107.9 (8)
C(1)-C(2)-Be(1)	68.1 (1)	H(5)-B(5)-H(4-5)	106.5 (18)
C(1)-C(2)-H(7)	132.3 (15)	H(5)-B(5)-H(2-5)	104.9 (17)
C(3)-C(2)-Be(1)	67.9 (1)	Be(1)-C(4)-H(9)	128.3 (19)
C(3)-C(2)-H(7)	119.6 (15)	C(2)-C(3)-C(4)	108.1 (2)
Be(1)-C(2)-H(7)	124.0 (16)	C(2)-C(3)-Be(1)	68.7 (1)
C(1)-C(5)-C(4)	107.3 (2)	C(2)-C(3)-H(8)	126.1 (19)
C(1)-C(5)-Be(1)	68.1 (1)	C(4)-C(3)-Be(1)	68.1 (1)
C(1)-C(5)-H(10)	117.5 (14)	C(4)-C(3)-H(8)	125.7 (19)
C(4)-C(5)-Be(1)	67.6 (1)	Be(1)-C(3)-H(8)	125.8 (19)
C(4)-C(5)-H(10)	135.0 (13)	C(1)-Be(1)-C(2)	43.2 (1)
Be(1)-C(5)-H(10)	125.5 (14)	C(1)-Be(1)-C(5)	43.4 (1)
C(5)-C(4)-C(3)	108.2 (2)	C(1)-Be(1)-C(4)	73.6 (1)
C(5)-C(4)-Be(1)	68.7 (1)	C(1)-Be(1)-C(3)	73.4 (1)
C(5)-C(4)-H(9)	125.5 (17)	C(1)-Be(1)-B(2)	147.2 (2)
C(5)-C(4)-Be(1)	68.5 (2)	C(1)-Be(1)-B(3)	124.7 (2)
C(5)-C(4)-H(9)	126.4 (17)	C(2)-Be(1)-C(3)	73.5 (1)
C(4)-Be(1)-B(3)	132.3 (2)	C(2)-Be(1)-C(4)	73.7 (1)
C(3)-Be(1)-B(2)	117.9 (2)	C(2)-Be(1)-C(3)	43.4 (1)
C(3)-Be(1)-B(3)	161.6 (2)	C(2)-Be(1)-B(2)	122.4 (2)
B(2)-Be(1)-B(3)	49.8 (1)	C(2)-Be(1)-B(3)	151.9 (2)
B(1)-B(2)-B(3)	59.7 (1)	C(5)-Be(1)-B(4)	43.6 (1)
B(1)-B(2)-Be(1)	56.5 (1)	C(5)-Be(1)-C(3)	73.7 (1)
B(1)-B(2)-H(2)	124.7 (2)	C(5)-Be(1)-B(2)	164.0 (2)
B(1)-B(2)-H(5-2)	126.1 (11)	C(5)-Be(1)-B(3)	115.9 (1)
B(3)-B(2)-H(5-2)	102.1 (9)	C(4)-Be(1)-C(3)	43.6 (1)
B(3)-B(2)-B(5)	91.2 (1)	C(4)-Be(1)-B(2)	136.9 (2)
B(3)-B(2)-H(2)	134.8 (11)	B(3)-B(1)-H(1)	125.0 (14)
B(3)-B(2)-H(5-2)	110.2 (8)	B(4)-B(1)-H(5)	65.2 (1)
B(5)-B(2)-Be(1)	121.0 (2)	B(4)-B(1)-H(1)	135.3 (13)
B(5)-B(2)-H(2)	131.2 (11)	B(5)-B(1)-H(1)	137.0 (14)
B(5)-B(2)-H(5-2)	46.3 (10)	B(1)-B(3)-B(2)	59.3 (1)
Be(1)-B(2)-H(2)	96.4 (11)	B(1)-B(3)-B(4)	56.6 (1)
Be(1)-B(2)-H(5-2)	90.3 (10)	B(1)-B(3)-Be(1)	123.7 (2)
H(2)-B(2)-H(5-2)	111.0 (13)	B(1)-B(3)-H(3)	131.8 (11)
B(2)-B(1)-B(3)	51.0 (1)	B(1)-B(3)-H(3-4)	99.2 (10)
B(2)-B(1)-B(4)	97.4 (2)	B(2)-B(3)-B(4)	91.1 (1)
B(2)-B(1)-B(5)	65.3 (1)	B(2)-B(3)-Be(1)	64.8 (1)
B(2)-B(1)-H(1)	126.4 (14)	B(2)-B(3)-H(3)	138.0 (11)
B(3)-B(1)-B(4)	65.2 (1)	B(2)-B(3)-H(3-4)	108.2 (9)
B(3)-B(1)-B(5)	97.3 (2)	B(4)-B(3)-Be(1)	120.7 (2)
B(3)-B(1)-H(5)	88.6 (1)	B(4)-B(3)-H(3)	130.0 (11)
B(3)-B(4)-H(4)	135.4 (11)	B(4)-B(3)-H(3-4)	43.4 (10)
B(3)-B(4)-H(3-4)	44.1 (9)	Be(1)-B(3)-H(3)	94.6 (11)
B(3)-B(4)-H(4-5)	104.1 (9)	Be(1)-B(3)-H(3-4)	91.8 (10)
B(5)-B(4)-H(4)	135.9 (11)	H(3)-B(3)-H(3-4)	108.6 (14)
B(5)-B(4)-H(3-4)	106.7 (9)	B(1)-B(4)-B(3)	58.2 (1)
B(5)-B(4)-H(4-5)	45.9 (9)	B(1)-B(4)-B(5)	57.0 (1)
H(4)-B(4)-H(3-4)	108.3 (14)	B(1)-B(4)-H(4)	137.1 (11)
H(4)-B(4)-H(4-5)	109.5 (15)	B(1)-B(4)-H(3-4)	101.4 (9)
H(5-2)-B(4)-H(4-5)	88.3 (13)	B(1)-B(4)-H(4-5)	101.5 (10)
B(1)-B(5)-B(2)	58.3 (1)	H(4-5)-B(5)-H(2-5)	90.2 (12)
B(1)-B(5)-B(4)	57.7 (1)	B(3)-H(3-4)-B(4)	92.6 (14)
B(1)-B(5)-H(5)	141.9 (16)	B(4)-H(4-5)-B(5)	90.4 (14)
B(1)-B(5)-H(4-5)	100.0 (10)	B(2)-H(5-2)-B(5)	89.5 (13)
B(1)-B(5)-H(2-5)	101.8 (9)		

the base of the square pyramid and of H(1) and $(\text{C}_5\text{H}_5)\text{Be}$ toward one another is most likely due to electronic effects which have not yet been elucidated, as intermolecular distances are too great to cause packing distortions. The observed 4° tilt of the cyclopentadienyl hydrogens toward beryllium is consistent with the prediction of a calculation on $\text{C}_5\text{H}_5\text{BeH}^4$ that the compactness of the Be orbitals would cause such a distortion in order to maximize overlap of C_5H_5 orbitals with those on Be.

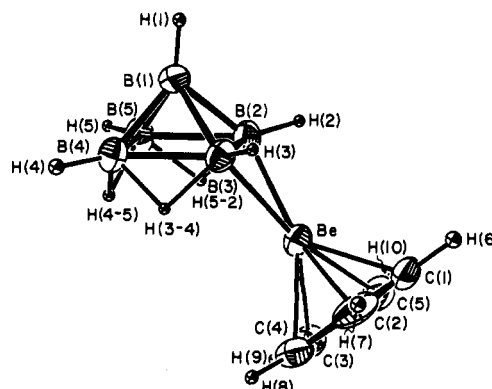


Figure 1. Low-temperature structure of $[\mu-(\eta^5\text{-C}_5\text{H}_5)\text{Be}]_2\text{B}_5\text{H}_8$. In this ORTEP drawing the nonhydrogen atoms are represented as 40% ellipsoids and the H atoms as 10% spheres.

Table III. Crystallographic Data for $[\mu-(\eta^5\text{-C}_5\text{H}_5)\text{Be}]_2\text{B}_5\text{H}_8$

mol wt	136.23
data collection temp, °C	-100
radiation (graphite monochromator)	Mo K α
scan speed, deg/min	2-24
range of 2θ , deg	3-50
total reflctns	1800
total independent reflctns	1709
total obsd reflctns	1294
cryst system	monoclinic
systematic abs	$h0l, l \text{ odd}; 0k0, k \text{ odd}$
space group	$P2_1/c$ (No. 14, second setting)
equiv positions	$x, y, z; \bar{x}, 1/2 + y, 1/2 + z;$ $x, 1/2 - y, 1/2 + z; \bar{x}, \bar{y}, \bar{z}$
no. of molecules/unit cell	4
$d(\text{calcd}), \text{g/cm}^3$	0.978
lattice constns (errors)	
$a, \text{\AA}$	10.266 (4)
$b, \text{\AA}$	5.616 (2)
$c, \text{\AA}$	16.187 (4)
β , deg	98.50 (30)
$V, \text{\AA}^3$	923.0 (5)
final discrepancy values	
data to parameter ratio (aniso)	5.9
R_1	0.0551
R_2	0.0831

The thermal stability of $[\mu-(\eta^5\text{-C}_5\text{H}_5)\text{Be}]_2\text{B}_5\text{H}_8$ is surprisingly high. It decomposes slowly at 80°C in C_6D_6 and rapidly at 140°C to uncharacterized insoluble materials. In di-*n*-butyl ether, however, there is no decomposition after several hours at 140°C . It did not react with dimethyl or diethyl ether at ambient temperature nor with dimethyl ether at 100°C in a benzene solution in sealed NMR tube experiments. No evidence of molecular rearrangement was obtained with these ethers. On the other hand, trimethylamine reacts rapidly, producing trimethylamine-borane as the only observable boron containing product. In contrast, 1,3-bis(dimethylamino)-naphthalene did not react upon heating to 100°C in C_6D_6 solution (or at ambient in diethyl ether), though it will deprotonate B_5H_9 in C_6D_6 solution at 60°C .⁵

Reaction of $[\mu-(\eta^5\text{-C}_5\text{H}_5)\text{Be}]_2\text{B}_5\text{H}_8$ with $(\text{CH}_3)_2\text{Zn}$ in diethyl ether appears to result in deprotonation to form CH_4 and what is tentatively characterized as $[\mu_{2,3}-(\eta^5\text{-C}_5\text{H}_5)\text{Be}](\mu_{3,4}\text{-CH}_3\text{Zn})\text{B}_5\text{H}_7$, whose ^{11}B NMR spectrum contains five equally intense doublets at $\delta -10.0, -12.4, -14.0, -17.8, -47.7$. These shifts are wholly consistent with the formulation, as the $[\mu-(\eta^5\text{-C}_5\text{H}_5)\text{Be}]$ gives rise to a large upfield shift to adjacent boron resonances, while the $(\mu\text{-CH}_3\text{Zn})$ group causes a downfield shift of all boron atoms in the cage, vide infra.

(4) Jemmis, E. D.; Alexandratos, S.; Schleyer, P. v. R.; Streitwieser, A.; Schaefer, H. F. *J. Am. Chem. Soc.* **1978**, *100*, 5695-5700.

(5) Gaines, D. F.; Jorgenson, M. W., unpublished results.

Table IV. Final Atomic Positional Parameters and Isotropic Thermal Parameters (\AA^2) for $[\mu-(\eta^5\text{-C}_5\text{H}_5)\text{Be}]_2\text{B}_5\text{H}_8$

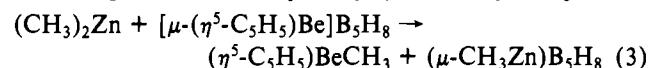
atom	10^4x	10^4y	10^4z	B_{iso}
C(1)	3530 (2)	1704 (4)	3684 (1)	
C(2)	2194 (2)	1674 (4)	3747 (1)	
C(5)	4074 (2)	3827 (4)	4029 (1)	
C(4)	3053 (3)	5132 (4)	4299 (1)	
C(3)	1897 (2)	3800 (5)	4128 (1)	
B(1)	2025 (2)	6727 (4)	1260 (1)	
B(2)	1479 (2)	5710 (4)	2135 (1)	
B(3)	3146 (2)	6001 (4)	2107 (1)	
B(4)	2993 (2)	4406 (4)	1118 (1)	
B(5)	1256 (2)	4114 (4)	1151 (1)	
Be(1)	2662 (2)	4383 (4)	3159 (1)	
H(1)	1891 (21)	8329 (44)	1022 (15)	4.6 (5)
H(2)	765 (19)	6606 (35)	2475 (14)	3.6 (5)
H(3)	3942 (19)	6934 (35)	2426 (13)	3.4 (4)
H(4)	3631 (18)	3928 (36)	705 (13)	3.1 (4)
H(5)	468 (25)	3217 (50)	775 (18)	6.3 (7)
H(3-4)	3565 (19)	4058 (36)	1846 (14)	3.5 (5)
H(4-5)	2260 (20)	2700 (39)	1215 (12)	3.7 (5)
H(5-2)	1103 (18)	3627 (36)	1922 (13)	3.3 (4)
H(6)	3958 (19)	560 (38)	3406 (14)	3.4 (5)
H(7)	1519 (22)	632 (44)	3544 (16)	4.6 (6)
H(10)	5608 (24)	4146 (42)	3996 (16)	5.0 (6)
H(9)	3143 (28)	6709 (58)	4561 (21)	7.3 (8)
H(8)	1093 (27)	4276 (51)	4216 (19)	6.5 (7)

Table V. Anisotropic Thermal Parameters^a ($\times 10^3$) for $[\mu-(\eta^5\text{-C}_5\text{H}_5)\text{Be}]_2\text{B}_5\text{H}_8$

atom	U_{11}	U_{22}	U_{33}	U_{12}	U_{13}	U_{23}
C(1)	38 (1)	39 (1)	38 (1)	8 (1)	3 (1)	3 (1)
C(2)	39 (1)	45 (1)	42 (1)	-5 (1)	2 (1)	16 (1)
C(5)	38 (1)	51 (1)	36 (1)	-7 (1)	-5 (1)	5 (1)
C(4)	93 (2)	38 (1)	23 (1)	7 (1)	3 (1)	-1 (1)
C(3)	51 (1)	72 (2)	38 (1)	25 (1)	22 (1)	22 (1)
B(1)	58 (2)	31 (1)	29 (1)	-1 (1)	8 (1)	4 (1)
B(2)	35 (1)	39 (1)	28 (1)	6 (1)	6 (1)	0 (1)
B(3)	40 (1)	37 (1)	28 (1)	-11 (1)	9 (1)	-5 (1)
B(4)	37 (1)	42 (1)	31 (1)	-8 (1)	9 (1)	-8 (1)
B(5)	32 (1)	43 (1)	31 (1)	-1 (1)	1 (1)	-2 (1)
Be(1)	32 (1)	38 (1)	25 (1)	0 (1)	6 (1)	0 (1)

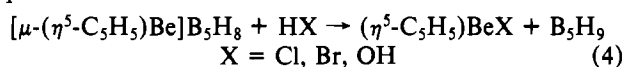
^a Of the form $\exp[-2\pi^2(U_{11}h^2a^{*2} + U_{22}k^2b^{*2} + U_{33}l^2c^{*2} + 2U_{12}hka^*b^* + 2U_{13}hla^*c^* + U_{23}klb^*c^*)]$.

The reaction of $(\text{CH}_3)_2\text{Zn}$ with the title compound in C_6D_6 solution is very different. First, the reaction is very slow, requiring more than 1 month to reach completion in the dark. The reaction is much faster in the presence of light but is then complicated by a side reaction that produces significant quantities of a metal, presumably zinc. Second, the ^{11}B NMR spectrum of the product contains three doublets in 2:2:1 ratio at δ -9.1, -19.3, and -48.5, respectively. A mass spectrum was not obtained owing to the low volatility of the product, but the formation of $(\eta^5\text{-C}_5\text{H}_5)\text{BeCH}_3$ in the reaction leads us to postulate that, in the absence of a basic solvent, the reaction produces $(\mu\text{-CH}_3\text{Zn})\text{B}_5\text{H}_8$ according to eq 3. A



similar compound, $\mu, \mu'\text{-Hg}(\text{B}_5\text{H}_8)_2$, having a similar ^{11}B NMR spectrum has recently been reported.⁶ Other synthetic routes to the largely unstudied zinc-borane clusters are under investigation.

Brønsted acids react rapidly and cleanly with the title compound in nonbasic solvents to produce B_5H_9 according to eq 4.



In aromatic solvents such as C_6D_6 , insoluble orange-brown solids form, suggesting the formation of solvated salts such as $(\text{C}_5\text{H}_5)\text{Be}(\text{C}_6\text{D}_6)^+\text{X}^-$, which have been described elsewhere.^{7a} Upon standing for 1 week, B_5H_9 had undergone exchange with the C_6D_6 to form $1\text{-DB}_5\text{H}_8$, presumably catalyzed by a beryllium complex ($1\text{-DB}_5\text{H}_8$ has been prepared from B_5H_9 and C_6D_6 in the presence of AlCl_3 ^{7b}).

Experimental Section

All manipulations of beryllium-containing materials were performed in a glovebag in a fume hood or in a glass high-vacuum system.⁸ Beryllium chloride was vacuum sublimed before use. Methylene chloride was distilled from 3- \AA molecular sieves, and other solvents were distilled from LiAlH_4 . All the beryllium- and boron-containing materials discussed are expected to be air- and moisture-sensitive, toxic, and in some cases pyrophoric. The NMR spectra were obtained with a Bruker WH-270 (^1H at 270 MHz, ^{11}B at 86.7 MHz⁹) spectrometer. Samples were contained in sealed 5-mm o.d. NMR tubes.

Infrared spectra were obtained on a Perkin-Elmer 700 spectrophotometer. Routine samples were obtained in the gas phase in a 10-cm cell with NaCl windows. Spectra for samples of very low vapor pressure were obtained by condensing the sample as a film on a polycrystalline ZnS window cooled to -196°C which was mounted inside a vacuum IR cell having NaCl windows.

Mass spectra were obtained on an AEI MS-902 spectrometer. Samples were introduced directly as a vapor from a vacuum flask equipped with O-ring stopcocks.

Preparation of $[\mu-(\eta^5\text{-C}_5\text{H}_5)\text{Be}]_2\text{B}_5\text{H}_8$. The reaction of a stirred pentane slurry of 10 mmol of KB_5H_8 ¹⁰ with excess $\text{C}_5\text{H}_5\text{BeCl}$,¹¹ while the reaction mixture was warmed from -40°C to ambient, produced high yields of $[\mu-(\eta^5\text{-C}_5\text{H}_5)\text{Be}]_2\text{B}_5\text{H}_8$, which was purified by high-vacuum trap-to-trap fractionation. The compound is a colorless solid of low volatility ($\text{vp} \ll 1$ torr at ambient) which melts at ca. 38°C . Its mass spectrum was as expected, exhibiting a mass cutoff at m/e 137. The exact mass of the parent was 137.1600 compared to 137.1605 calculated for $^{12}\text{C}_5^{11}\text{B}_5^9\text{Be}_1^1\text{H}_{13}$.

Reactions of the title compound were surveyed by ^1H and/or ^{11}B NMR analysis of reaction mixtures which were contained in sealed 5-mm NMR tubes. In most cases the reactions were clean enough that all the major boron-containing products could be unequivocally identified by their characteristic ^{11}B NMR spectra. A typical example is the quantitative reaction of the title compound with Brønsted acids as shown in eq 4. Several reactions were also characterized by other means as indicated below.

Reactions of $[\mu-(\eta^5\text{-C}_5\text{H}_5)\text{Be}]_2\text{B}_5\text{H}_8$ with $(\text{CH}_3)_2\text{Zn}$. In a C_6D_6 solution, equimolar mixtures required about 1 month to reach completion according to eq 3. The ^{11}B NMR spectrum was consistent with that expected for $(\mu\text{-CH}_3\text{Zn})\text{B}_5\text{H}_8$, vide supra. When the reaction was carried out in the absence of solvent, the same borane product was observed and the $(\eta^5\text{-C}_5\text{H}_5)\text{BeCH}_3$ was separated and identified by its infrared spectrum. In diethyl ether solution, reaction occurred immediately upon warming to room temperature. The basic solvent led to the formation of a very different product, tentatively identified as $[\mu_{2,3}(\eta^5\text{-C}_5\text{H}_5)\text{Be}](\mu_{3,4}\text{-CH}_3\text{Zn})\text{B}_5\text{H}_7$ on the basis of its ^{11}B spectrum.

X-ray Structure Solution and Refinement. A single crystal of $[\mu-(\eta^5\text{-C}_5\text{H}_5)\text{Be}]_2\text{B}_5\text{H}_8$ was grown from a melt in a sealed evacuated Pyrex capillary on a Syntex PI autodiffractometer. The data set was not absorption corrected. The structure was solved by direct methods.^{12,13}

- (7) (a) Morgan, F. L.; McVicker, G. B. *J. Am. Chem. Soc.* **1968**, *90*, 2789-2792. (b) Heppert, J. A.; Gaines, D. F., unpublished results.
- (8) Shriver, D. F. "Manipulation of Air-Sensitive Compounds"; McGraw-Hill: New York, 1969.
- (9) The ^{11}B chemical shifts are relative to $\text{BF}_3\cdot\text{OEt}_2$ with negative signs indicating upfield shifts.
- (10) Brice, V. T.; Shore, S. G. *Inorg. Chem.* **1973**, *12*, 309.
- (11) Bartke, T. C.; Bjørseth, A.; Haaland, A.; Marstokk, K. M.; Mollendal, H. *J. Organomet. Chem.* **1975**, *85*, 271.
- (12) Germain, G.; Main, P.; Woolfson, M. M. *Acta Crystallogr., Sect. B* **1974**, *B26*, 274-285.
- (13) Computer programs used in the structural analysis were written by J.C.C. Plots were made with use of C. K. Johnson's ORTEP.

Following several cycles of full-matrix least-squares refinement, in which positional and isotropic thermal parameters were varied for the nonhydrogen atoms, a difference map revealed the hydrogen positions. Additional least-squares refinement, in which the nonhydrogen atoms were allowed to vary in both positional and anisotropic thermal parameters, converged at $R_1 = 0.0551^{14}$ and $R_2 = 0.0831^{15}$. Scattering factors used were those of Hanson et al.,¹⁶ and the least-squares refinement was based on minimization of $\sum w_2(|F_o| - |F_c|)^2$, with weights w_i equal to $1/\sigma(F_o)^2$. Estimated standard deviations in bond lengths (Table I) and angles (Table II), positional parameters

$$(14) R_1 = \sum (|F_o| - |F_c|) / |F_o|$$

$$(15) R_2 = [\sum w_i (|F_o| - |F_c|)^2 / \sum |F_o|^2]^{1/2}, \text{ where } w_i = 1/\sigma(F_o)^2.$$

(16) Hanson, H. P.; Herman, F.; Lea, J. D.; Skillman, S. *Acta Crystallogr.* 1964, 17, 1040-1044.

and isotropic thermal parameters (Table IV), and anisotropic thermal parameters (Table V) were calculated from a full variance-covariance matrix in the final cycle of least-squares refinement.

Acknowledgment. This work was supported in part by grants, including departmental instrument grants for X-ray and NMR facilities, from the National Science Foundation.

Registry No. $[\mu-(\eta^5\text{-C}_5\text{H}_5)\text{Be}]_2\text{B}_5\text{H}_8$, 71163-79-6; $[\mu_{2,3}-(\eta^5\text{-C}_5\text{H}_5)\text{Be}](\mu_{3,4}\text{-CH}_3\text{Zn})\text{B}_5\text{H}_7$, 77123-44-5; $(\mu\text{-CH}_3\text{Zn})\text{B}_5\text{H}_8$, 77123-45-6; $(\text{CH}_3)_2\text{Zn}$, 544-97-8; $\text{C}_5\text{H}_5\text{BeCl}$, 36346-97-1; KB_5H_8 , 56009-95-1.

Supplementary Material Available: Tables of observed and calculated structure factor amplitudes (8 pages). Ordering information is given on any current masthead page.

Contribution from the Department of Chemistry,
University of Nebraska, Lincoln, Nebraska 68588

Variations in Platinum-Carbon (sp^3) Bond Lengths. Crystal and Molecular Structure of (1,5-Cyclooctadiene)(η^1 -cyclopentadienyl)methylplatinum(II), $\text{Pt}(\text{1,5-C}_8\text{H}_{12})(\eta^1\text{-C}_5\text{H}_5)(\text{CH}_3)$

CYNTHIA S. DAY,^{1a} VICTOR W. DAY,^{*1a} ALAN SHAVER,^{*1b} and HOWARD C. CLARK^{1c}

Received December 9, 1980

The crystal and molecular structure of the title compound has been determined by X-ray diffraction methods. The complex crystallizes in the monoclinic space group $P2_1/n$ with $Z = 4$ and cell dimensions $a = 6.589$ (1) Å, $b = 12.187$ (2) Å, $c = 15.447$ (2) Å, and $\beta = 95.30$ (1)°. The observed and calculated densities were 2.049 and 2.062 g/cm³, respectively. The structure has been refined to a final R factor on F of 0.037 for 15 anisotropic nonhydrogen atoms and 2606 absorption corrected ($\mu r = 2.09$) reflections having $I > 3\sigma(I)$. The structure consists of discrete molecules with a square-planar arrangement of the carbon ligands. The platinum-methyl bond distance (2.068 (8) Å) is significantly shorter than the platinum-Cp distance (2.151 (8) Å). The platinum-olefin distance trans to the Cp ligand is shorter than the one trans to the methyl group. These facts are consistent with the previous observation that the NMR trans influence of the Cp ligand is much smaller than that of the methyl group. The differences in the bonding of the two sp^3 -hybridized carbons are discussed in terms of σ - π hyperconjugation of the Pt-Cp bond with the diene.

Introduction

Recently the title compound (**1**) was prepared and some of its reactions reported.² This complex undergoes a Diels-Alder addition of hexafluoro-2-butyne in which the acetylene adds to the Cp ring (Cp = C_5H_5) trans to the platinum atom substituent.³ This was taken to imply that the metal does not take part in the mechanism of the addition other than possibly acting as a bulky steric hindrance to the approach on one side of the Cp ring. This is in contrast to "metal-assisted" cycloaddition reactions observed in some iron⁴ and nickel⁵ systems. It was of interest, therefore, to determine the structure of **1** to establish if there was any unusual steric feature that might prevent precoordination of an acetylene.

Also of interest was the comparison of the Pt-CH₃ and Pt-(η^1 -Cp) bond distances. A priori, they would be predicted to be very similar since both are single bonds to sp^3 carbon atoms. However, the Mo-CH₃ bond distance in $(\eta^5\text{-Cp})_2\text{Mo}(\text{NO})\text{CH}_3$ is about 0.1 Å shorter than the Mo-(η^1 -Cp) bond distance in $\text{Cp}_3\text{Mo}(\text{NO})$.⁶ The title complex is an ideal

model to investigate the generality of such differences since both types of ligands, CH₃ and η^1 -Cp, are in the same complex, and they are situated trans to identical olefin ligands.

There is spectroscopic evidence that a significant difference in the bonding of the methyl and Cp groups exists in **1**. NMR coupling constants are often used to estimate the relative trans influences of different groups in platinum complexes.⁷ Comparison of the $J(\text{Pt-C})$ and $J(\text{Pt-H})$ values for the COD group (COD = 1,5-cyclooctadiene) trans to the methyl and Cp ligands indicated that the NMR trans influence of the latter was much less than that of the methyl group.² This seems inconsistent with both groups being bound to the platinum atom by identical metal-carbon (sp^3) bonds, particularly, since other NMR studies have shown there is little or no discrimination among sp^3 -hybridized carbon ligands.⁸

Experimental Section

Large, well-shaped, yellow single crystals of **1** suitable for X-ray studies were grown from diethyl ether at -20 °C. Weissenberg and precession photographs were used to determine the probable space group and a preliminary set of lattice constants indicated monoclinic, $2/m$, symmetry. The systematically absent reflections were those uniquely required by the centrosymmetric space group, $P2_1/n$ (a special

(1) (a) University of Nebraska. (b) Department of Chemistry, McGill University, 801 Sherbrooke St. W., Montreal, Quebec, Canada H3A 2K6. (c) University of Guelph, Guelph, Ontario, Canada N1G 2W1.

(2) H. C. Clark and A. Shaver, *Can. J. Chem.*, **54**, 2068 (1976).

(3) H. C. Clark, D. G. Ibbott, N. C. Payne, and A. Shaver, *J. Am. Chem. Soc.*, **97**, 3555 (1975).

(4) R. E. Davis, T. A. Dodds, T.-H. Hseu, J. C. Wagnong, T. Devon, J. Tancrede, J. S. McKennis, and R. Pettit, *J. Am. Chem. Soc.*, **96**, 7562 (1974).

(5) D. W. McBride, E. Dukek, and F. G. A. Stone, *J. Chem. Soc.*, 1752 (1964).

(6) F. A. Cotton and G. A. Rusholme, *J. Am. Chem. Soc.*, **94**, 402 (1972).

(7) T. G. Appleton, H. C. Clark, and L. E. Manzer, *Coord. Chem. Rev.*, **10**, 335 (1973).

(8) (a) M. R. Collier, C. Eaborn, B. Jovanovic, M. F. Lappert, Lj. Manojlovic-Muir, K. W. Muir, and M. M. Trudlock, *J. Chem. Soc., Chem. Commun.*, 613 (1972). (b) C. J. Cardin, D. J. Cardin, M. F. Lappert, and K. W. Muir, *J. Chem. Soc., Dalton Trans.*, 46 (1978).